ChemPubSoc Europe

DOI: 10.1002/chem.201500290

CHEMISTRY
A European Journal
Full Paper

Bond Cleavage

The Mechanism of N–O Bond Cleavage in Rhodium-Catalyzed C–H Bond Functionalization of Quinoline *N*-oxides with Alkynes: A Computational Study

Yingzi Li,[a] Song Liu,[a] Zisong Qi,[b] Xiaotian Qi,[a] Xingwei Li,*[b] and Yu Lan*[a]

Abstract: Metal-catalyzed C–H activation not only offers important strategies to construct new bonds, it also allows the merge of important research areas. When quinoline *N*-oxide is used as an arene source in C–H activation studies, the N–O bond can act as a directing group as well as an O-atom donor. The newly reported density functional theory method, M11L, has been used to elucidate the mechanistic details of the coupling between quinoline N–O bond and alkynes, which results in C–H activation and O-atom transfer. The computational results indicated that the most favorable pathway involves an electrophilic deprotonation, an insertion of an acetylene group into a Rh–C bond, a reductive elimination to form an oxazinoquinolinium-coordinated Rh^{I} intermediate, an oxidative addition to break the N–O bond, and a protonation reaction to regenerate the active catalyst. The regioselectivity of the reaction has also been studied by using prop-1-yn-1-ylbenzene as a model unsymmetrical substrate. Theoretical calculations suggested that 1-phenyl-2-quinolinylpropanone would be the major product because of better conjugation between the phenyl group and enolate moiety in the corresponding transition state of the regioselectivity-determining step. These calculated data are consistent with the experimental observations.

Introduction

Transition-metal-catalyzed C–H bond cleavage and functionalization reactions have been extensively explored over the past three decades to provide advantageous strategies for the formation of new C–X bonds (X = C, N, O, S) that are both atom-economical and waste-reducing.[1] Numerous transition metals have been employed to catalyze C–H functionalization reactions, including palladium,[2] nickel,[3] ruthenium,[4] rhodium,[5] and iron complexes.[6] The $[Rh^{III}Cp^*]$ (Cp* = pentamethylcyclopentadienyl) complex is of particular interest to serve this purpose, and has been studied experimentally and theoretically.[5h,7] Notably, Li et al.[8] and Chang et al.[9] independently reported the $[Rh^{III}Cl_2Cp^*]_2$-catalyzed C–H bond functionalization of quinoline *N*-oxide with alkynes (Scheme 1), which represents a powerful strategy that combines C–H activation and O-atom transfer and leads to efficient synthesis of substituted acetophenones. In this particular reaction, the *N*-oxide moiety served as a directing group, which led to the regioselective activation of the C8–H bond.[10] Effects similar to this have also been recently reported when using several other metal catalysts.[11] Notably, the *N*-oxide moiety can also be used as an oxidant to keep the reaction redox-neutral overall for the release of the coupled product through the cleavage of the N–O bond.[12]

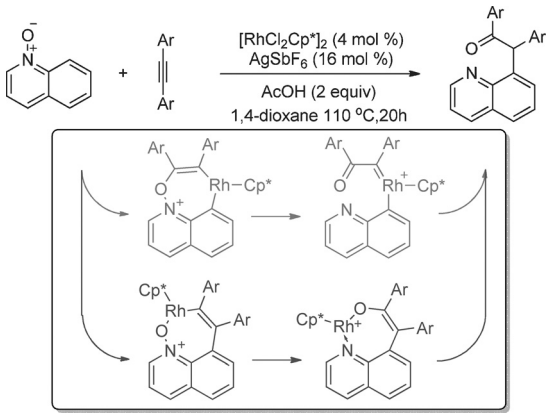

Scheme 1. $[Rh^{III}Cl_2Cp^*]_2$-catalyzed C–H bond functionalization and N–O bond cleavage of quinoline *N*-oxide with alkynes.

As part of our ongoing work towards elucidation of the mechanisms of transition-metal-catalyzed reactions, we developed a keen interest in exploring the mechanism of this N–O cleavage process.[8,9] As shown in Scheme 1, following the initial C–H bond cleavage, the N–O bond of the quinoline *N*-

[a] *Y. Li,[+] S. Liu,[+] X. Qi, Prof. Dr. Y. Lan*
School of Chemistry and Chemical Engineering
Chongqing University
Chongqing 400030 (China)
E-mail: lanyu@cqu.edu.cn

[b] *Z. Qi, Prof. Dr. X. Li*
Dalian Institute of Chemical Physics
Chinese Academy of Sciences
Dalian 116023 (China)
E-mail: xwli@dicp.ac.cn

[+] *These authors contributed equally to this work.*

Supporting information for this article is available on the WWW under http://dx.doi.org/10.1002/chem.201500290.

oxide substrate might undergo an O-atom transfer to the C≡C triple bond to afford an α-oxo carbenoid species (red pathway).[8,9] It is worth noting that similar processes have been reported with gold,[13] iridium,[10c,14] and ruthenium catalysts,[15] although this pathway is rare in rhodium-catalyzed reactions.[10d] Alternatively, the N–O cleavage may occur through oxidative addition of Rh^{I} to form a quinoline-tethered Rh^{III} enolate intermediate (blue pathway).[12,16] Given the complexity of the [Rh^{III}Cp*]-catalyzed C–H bond functionalization of quinoline *N*-oxide with alkynes, we performed density functional theory (DFT) calculations to elucidate the mechanism of this type of reaction and provide greater clarity with regard to the function and the fate of this polar N–O bond.

Computational Methods

All of the DFT calculations conducted in this study were carried out by using the Gaussian 09 series of programs.[17] DFT method B3LYP[18] with a standard 6-311G(d) basis set (lanl2dz basis set for Rh) was used for the geometry optimizations. The M11L functional, proposed by Truhlar et al.,[19] was used with a 6-311+G(d) basis set (SDD basis set for Rh) to calculate the single-point energies because it was envisaged that this strategy would provide greater accuracy with regard to the energetic information.[20] The solvent effects were taken into consideration by using single-point calculations based on the gas-phase stationary points with a SMD continuum solvation model.[21] The energies presented in this paper are the M11L-calculated Gibbs free energies in a 1,4-dioxane solvent with B3LYP-calculated thermodynamic corrections.

Results and Discussion

As shown in Scheme 2, four possible pathways were taken into account during our computational modeling of this reaction (i.e., paths a–d). All these four pathways begin with the coordination of quinoline *N*-oxide to Rh^{III} precursor **A**,[22] which is followed by an *N*-oxide-directed electrophilic deprotonation by acetate and coordination of acetylene substrate to give rhodacycle **B**. The subsequent insertion of the acetylene substrate into the Rh–C bond of intermediate **B** gives intermediate **C**, which is a common intermediate for both paths a and c. In path a (blue pathway), complex **C** is proposed to undergo a reductive elimination reaction to form a new C–O bond in π-coordinated complex **D**. The N–O bond in complex **D** would then oxidatively add back to Rh^{I} to generate Rh^{III} enolate intermediate **E**. Protonolysis of intermediate **E** by acetic acid would release one molecule of product **F** and regenerate complex **A**. Product **F** could also be generated by the protonation of intermediate **G**, which is an isomer of intermediate **E**. In path c (green pathway), the migration of the oxygen atom from complex **C** would lead to the formation of Rh^{V} oxo intermediate **J**. A subsequent oxygen insertion reaction may give rise to intermediate **E**, which is the common intermediate in path a. Alternatively, the insertion of the acetylene substrate into the Rh–O bond of intermediate **B** would give rise to a common intermediate **H**, which could proceed along path b or path d. For path b (red pathway), cleavage of the N–O bond would lead to the formation of α-oxo carbenoid species **I**, which could undergo carbene insertion to give intermediate **G**. This intermediate is either protonated directly or isomerizes to intermediate **E**, followed by protonolysis to afford product **F** together with the regeneration of active catalyst **A**. Intermediate **H** could also undergo reductive elimination through path d to give π-complex **D**. All four of these different pathways have been evaluated in the current study by using DFT calculations.

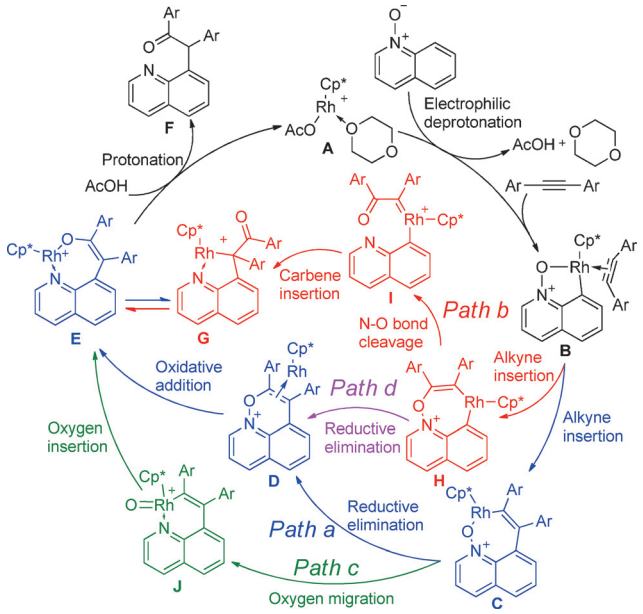

Scheme 2. Plausible mechanisms for the rhodium-catalyzed C–H bond functionalization and N–O bond cleavage of quinoline *N*-oxide with alkynes.

The free energy profiles for the initiation steps of the rhodium-catalyzed C–H bond functionalization and N–O bond cleavage of quinoline *N*-oxide with alkynes are shown in

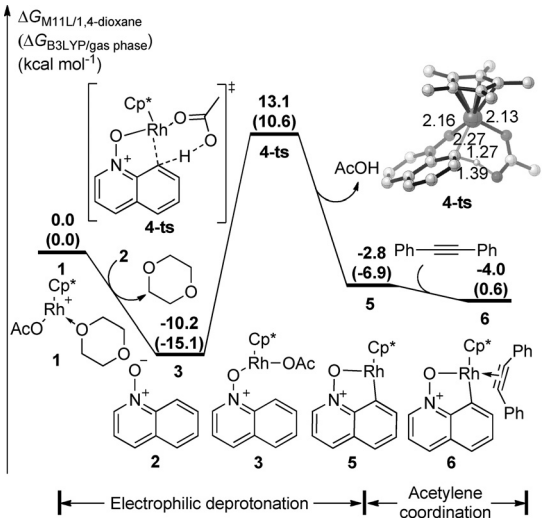

Figure 1. Free energy profiles for the initiation steps of the rhodium-catalyzed C–H bond functionalization and N–O bond cleavage of quinoline *N*-oxide with alkynes. Values are given in kcal mol^{-1} and represent the relative free energies calculated by the M11L method in 1,4-dioxane. The values given in parentheses are the relative free energies calculated by using the B3LYP method in the gas phase.

Figure 1. Rhodium acetate complex **1** was set to a relative zero value, and this complex could be generated from the $[RhCl_2Cp^*]_2$ catalyst through dissociation and ligand-exchange reactions in the presence of acetic acid and $AgSbF_6$.[22] The coordination of quinoline *N*-oxide to the catalyst leads to the formation of intermediate **3** in an exothermic process that releases 10.2 kcal mol^{-1} of free energy. The subsequent *N*-oxide-directed, acetate-assisted electrophilic deprotonation reaction takes place via transition state **4-ts** with an activation free energy of 23.3 kcal mol^{-1}. This step results in the formation of intermediate **5** together with the release of one molecule of acetic acid. The subsequent coordination of diphenylethyne to intermediate **5** gives complex **6**, which is the key species involved in all four possible pathways depicted in Scheme 2 (the corresponding complex **B**).

The free energy profiles of the N–O bond cleavage and C–C bond formation steps for all four possible pathways are given in Figure 2, starting from common intermediate **6**. For path a (blue pathway), the insertion of the acetylene substrate into the Rh–C bond takes place via transition state **7-ts** with an energetic span of 18.1 kcal mol^{-1}, which would lead to formation of rhodacyclic intermediate **8**. The overall process for the conversion of **6** to **8** is exothermic and releases 3.8 kcal mol^{-1} of free energy. A subsequent reductive elimination reaction leads to the reversible formation of oxazinoquinolinium-coordinated rhodium complex **10** via transition state **9-ts**. The energetic span for this step was determined to be 24.6 kcal mol^{-1}, which indicated that the reductive elimination would be the rate-limiting step for the whole catalytic cycle. An oxidative addition reaction would then lead to the cleavage of the N–O bond via transition state **11-ts**, which has an energetic span of as low as 2.1 kcal mol^{-1}. Transition state **11-ts** would lead to the irreversible formation of rhodium π-enolate complex **12** in an exothermic reaction that releases 62.6 kcal mol^{-1} of free energy. Complex **12** could then isomerize to carbon-coordinated rhodium complex **13**. Path c (green pathway) also starts from intermediate **8**. In this case, an oxygen transfer step would occur via transition state **19-ts** to form Rh^V oxo species **20**. The energetic span for this process was calculated to be as high as 45.8 kcal mol^{-1}, which is much higher than the energy required for the

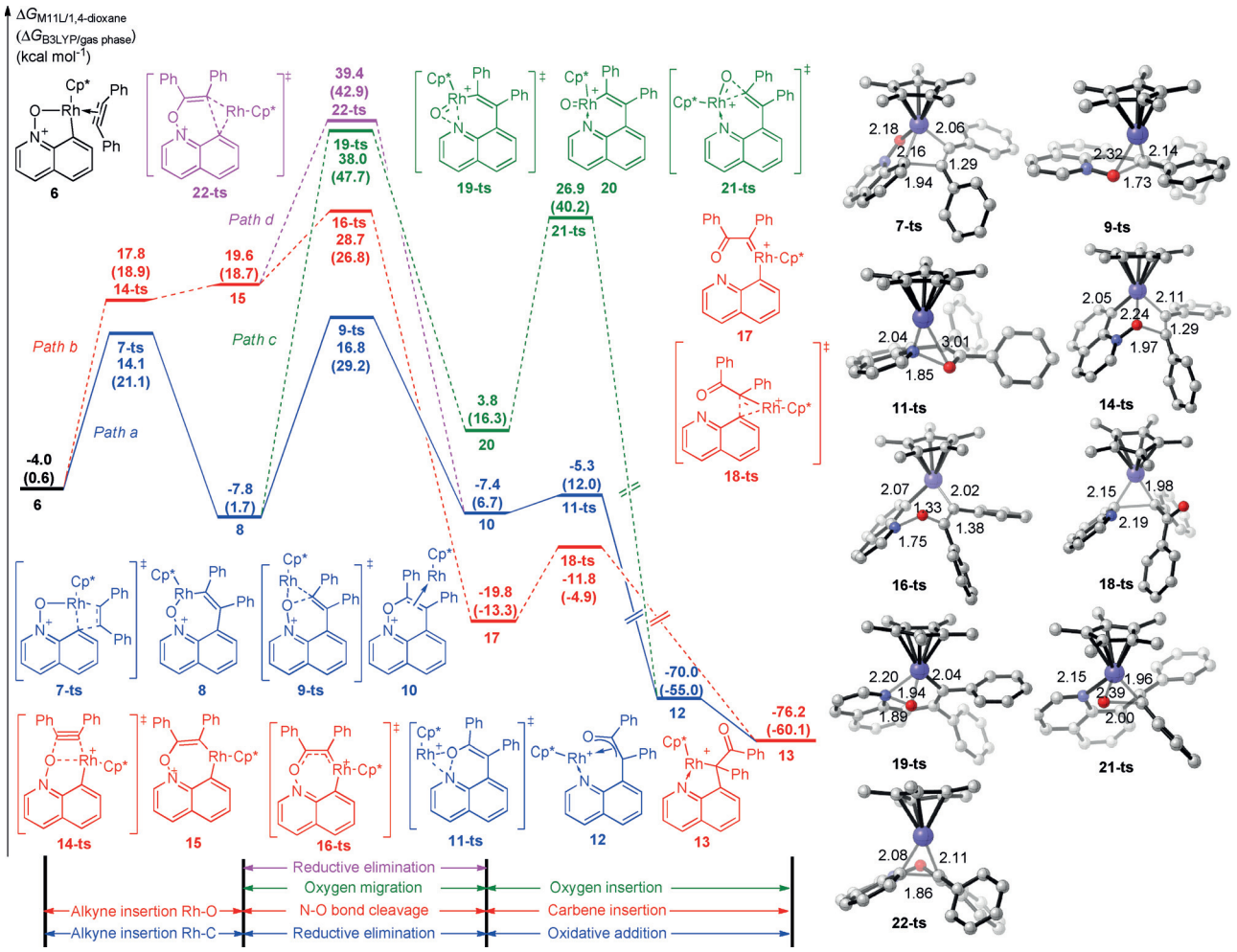

Figure 2. Free energy profiles for the N–O bond cleavage and C–C bond formation steps of the rhodium-catalyzed C–H bond functionalization and N–O bond cleavage of quinoline *N*-oxide with alkynes. Values are given in kcal mol^{-1} and represent the relative free energies calculated by using the M11L method in 1,4-dioxane. The values given in parentheses are the relative free energies calculated by using the B3LYP method in the gas phase. Values for the bond lengths given in the geometry information are reported in Å.

reductive elimination step via transition state **9-ts**. Based on these data, path c is unlikely because of its extremely high activation energy.

In path b (red pathway), the acetylene substrate would be reversibly inserted into the Rh–O bond via transition state **14-ts** with an activation free energy of 21.8 kcal mol^{-1}, which would lead to the formation of another rhodacyclic intermediate **15**. The subsequent cleavage of the N–O bond would take place via transition state **16-ts**, which leads to the irreversible formation of α-oxo carbenoid intermediate **17**. A migratory insertion of the aryl group into the carbene moiety would then take place via transition state **18-ts** with an activation free energy of only 8.0 kcal mol^{-1}. Common intermediate **13** could also be irreversibly generated by this pathway. A comparison of path b and path a revealed that the relative free energy of transition state **16-ts** was 11.9 kcal mol^{-1} higher than that of transition sate **9-ts**. Therefore, these results clearly show that path b is unfavorable. We also considered the reductive elimination of intermediate **15** (i.e., path d, pink). However, the relative free energy of transition state **22-ts** was determined to be as high as 39.4 kcal mol^{-1}, which is much higher than that of transition state **9-ts**. Taken together, it follows that path a is the most favorable pathway for this transformation.

Complex **12** and its isomer **13** are proposed to be protonolyzed by acetic acid. As shown in Figure 3, the coordination of acetic acid to complex **12** would lead to the formation of intermediate **23**. A subsequent intramolecular proton transfer from the acetate moiety to the enolate moiety would take place via transition state **24-ts** with an activation energy of 17.1 kcal mol^{-1}, which ultimately affords enol-coordinated rhodium intermediate **25**. After releasing one molecule of desired product **26**, active catalyst **1** would be regenerated. Complex **13** could also be protonated by acetic acid via transition state **28-ts**. The relative free energy for **28-ts** was determined to be only 0.1 kcal mol^{-1} higher than that of **24-ts**, which indicated that the protonation step could also occur via this pathway. The protonolysis of the carbon atom was also considered as a possible pathway. As shown in Figure 3, two possible transition states **29-ts** and **30-ts** were also located individually. However, the relative free energies for these two transition states were much higher than that of transition state **24-ts**.

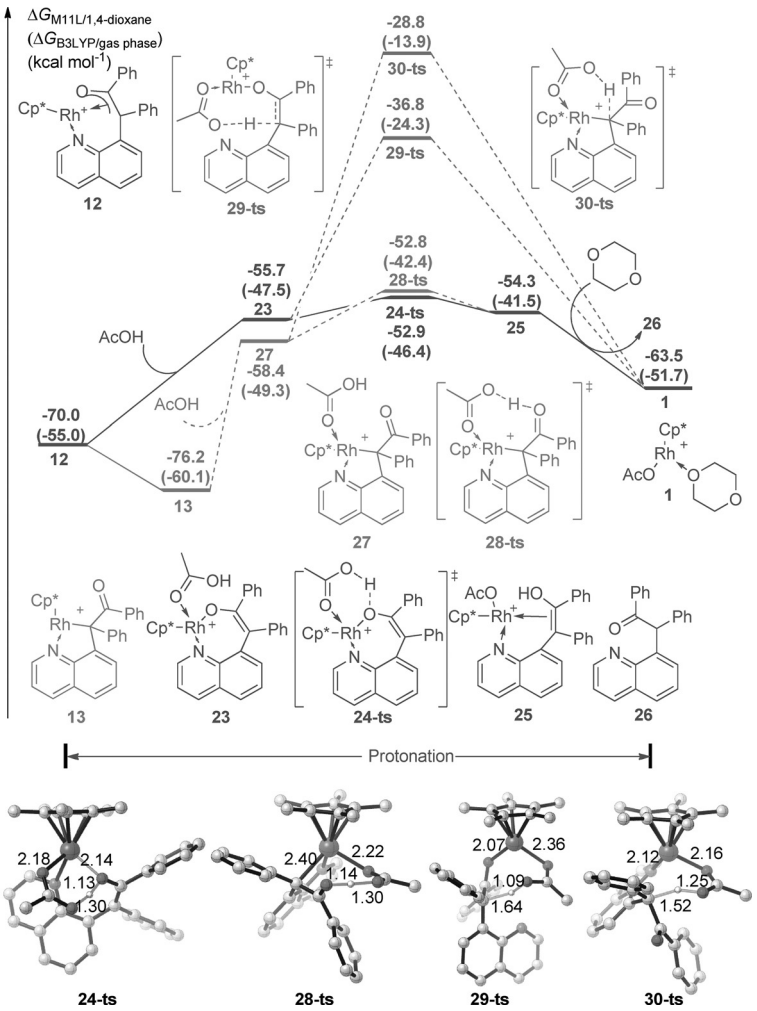

Figure 3. Free energy profiles for the protonation steps in the rhodium-catalyzed C–H bond functionalization and N–O bond cleavage of quinoline *N*-oxide with alkynes. The values are given in kcal mol^{-1} and represent the relative free energies calculated by using the M11L method in 1,4-dioxane. The values given in parentheses are the relative free energies calculated by using the B3LYP method in the gas phase. Values for the bond lengths in the geometry information are given in Å.

Thus, in our lowest-energy pathway, the rhodium-catalyzed C–H bond functionalization and the redox-neutral coupling between quinoline *N*-oxide and alkynes proceeds through an electrophilic deprotonation, followed by the insertion of the acetylene substrate into a Rh–C bond, a reductive elimination to form an oxazinoquinolinium-coordinated rhodium complex, an oxidative addition to break the N–O bond, and protonolysis to eventually regenerate the active catalyst.

As shown in Scheme 3, the use of the non-symmetrical alkyne substrate such as prop-1-yn-1-ylbenzene (**31**) under typical reaction conditions might result in the formation of two possible isomeric products **32** and **33**. However, only product **32** was isolated under the conditions shown in the scheme in a yield of 74%, whereas the other regioisomer (**33**) was not detected.[8,9] DFT calculations were also employed to study the regioselectivity of this reaction.

As shown in Figure 4, intermediate **34** would be formed by the coordination of prop-1-yn-1-ylbenzene (**31**) to common starting intermediate **5**. The insertion of the acetylene moiety would occur via transition state **35-ts** to give intermediate **36** with an energetic span of 18.5 kcal mol^{-1}. A subsequent reductive elimination reaction would then take place via transition state **37-ts** with an activation free energy of 25.3 kcal mol^{-1}, and the following processes would afford compound **32** as the major product. In contrast, the insertion of the acetylene substrate could occur via transition state **41-ts**. The corresponding reductive elimination reaction would then proceed through transition state **43-ts**, with subsequent processes that lead to

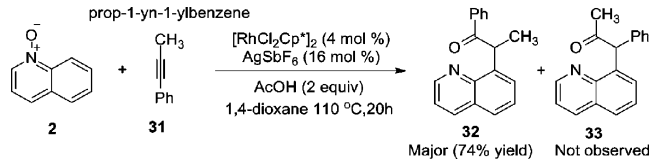

Scheme 3. $[Rh^{III}Cl_2Cp^*]_2$-catalyzed C–H bond functionalization and N–O bond cleavage of quinoline *N*-oxide with an asymmetric alkyne.

the formation of the other regioisomer **46** as the final product. Notably, this product was not observed experimentally. A comparison of the relative free energies of transition states **37-ts** and **43-ts** revealed that the latter was 8.0 kcal mol^{-1} higher in energy than the former. This result explains why complex **46** was not formed under the typical reaction conditions and is, therefore, consistent with the experimental observations. Data pertaining to the geometries of transition states **37-ts** and **43-ts** are shown in Figure 4. In transition state **37-ts**, the dihedral angle of the phenyl group and enolate moiety (C1-C2-C3-C4) was found to be 38.4°. However, in transition state **43-ts**, the phenyl group was almost perpendicular to the enolate moiety, with a resulting lack of conjugation that leads to the higher relative energy of transition state **43-ts**. This explains why compound **32** was isolated as the major product of this transformation.

Conclusion

The newly reported DFT method, M11L, has been used to clarify the mechanism of the rhodium-catalyzed C–H bond functionalization and N–O bond cleavage of quinoline *N*-oxide with acetylene reported by Li et al.[8] Our results show a clear preference for path a, which involves an electrophilic deprotonation, followed by the insertion of an acetylene substrate into a Rh–C bond, a reductive elimination to form an oxazinoquinolinium-coordinated rhodium complex, an oxidative addition to break the N–O bond, and a protonolysis to regenerate the active catalyst. For this pathway, the rate-determining step was found to be the reductive elimination, and the energetic span of this process is comparable to that of the C–H cleavage. The regioselectivity of the reaction with respect to the non-symmetrical substrate prop-1-yn-1-ylbenzene was also studied. Theoretical calculations indicated that 1-phenyl-2-quinolinylpropanone would be formed as the major product because of occurrence of better conjugation between the phenyl group and the enolate moiety in the transition state of the regiose-

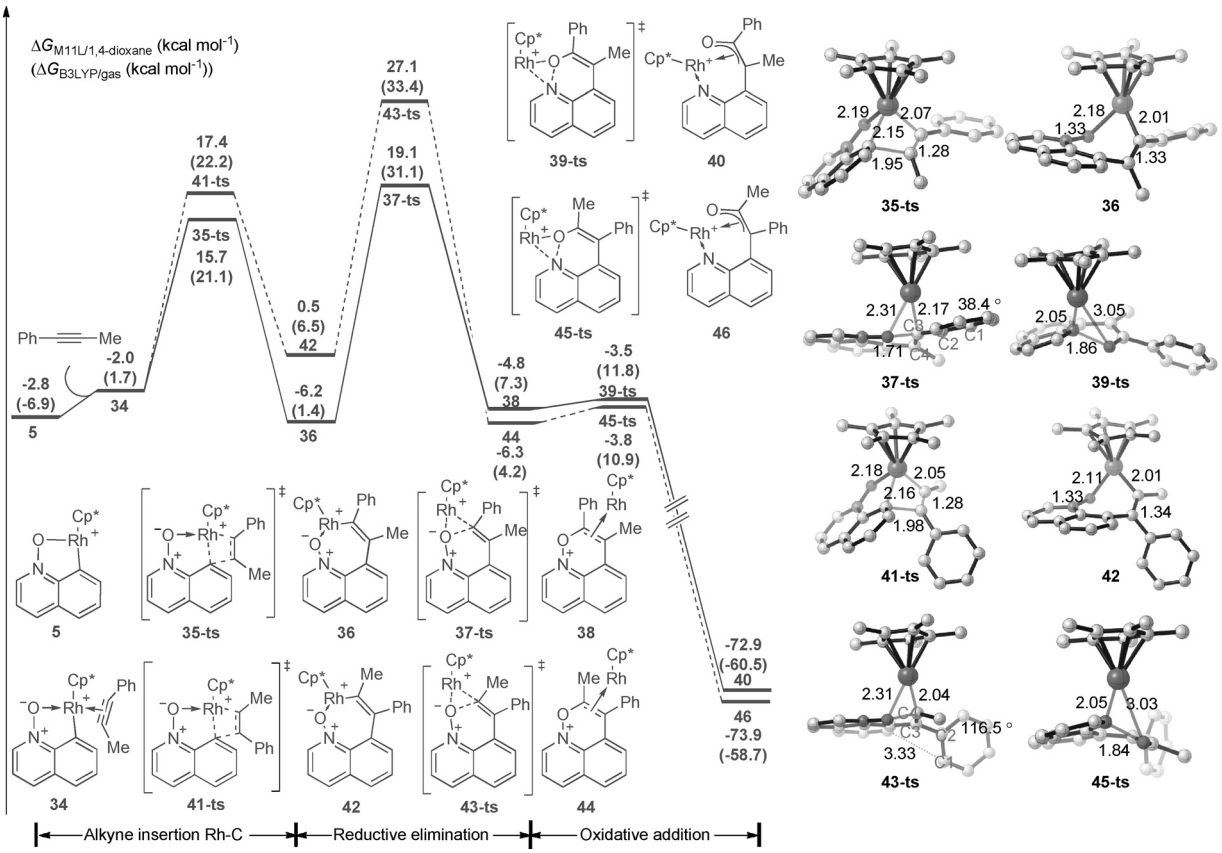

Figure 4. Free energy profile for the regioselectivity of the rhodium-catalyzed C–H bond functionalization and N–O bond cleavage of quinoline *N*-oxide with prop-1-yn-1-ylbenzene. Values are given in kcal mol^{-1} and represent the relative free energies calculated by using the M11L method in 1,4-dioxane. The values given in parentheses are the relative free energies calculated by using the B3LYP method in the gas phase. Values for the bond lengths in the geometry information section are given in Å.

lectivity-determining step. This result was consistent with the experimental observations.

Acknowledgements

This project was supported by the National Science Foundation of China (grants 21372266, 51302327, 21272231, 21272231, and 21472186) and the Foundation of 100 Young Chongqing University (project 0903005203191).

Keywords: C–H bond activation · cleavage reactions · density function calculations · quinolines · rhodium

[1] For selected reviews, see: a) L. Ackermann, *Chem. Rev.* **2011**, *111*, 1315 – 1345; b) J. F. Hartwig, *Chem. Soc. Rev.* **2011**, *40*, 1992 – 2002; c) W. R. Gutekunst, P. S. Baran, *Chem. Soc. Rev.* **2011**, *40*, 1976 – 1991; d) L. McMurray, F. O'Hara, M. J. Gaunt, *Chem. Soc. Rev.* **2011**, *40*, 1885 – 1898; e) M. C. Willis, *Chem. Rev.* **2010**, *110*, 725 – 748; f) D. Alberico, M. E. Scott, M. Lautens, *Chem. Rev.* **2007**, *107*, 174 – 238; g) E. M. Beck, M. J. Gaunt, *Top. Curr. Chem.* **2009**, *292*, 85 – 121; h) C.-L. Sun, B.-J. Li, Z.-J. Shi, *Chem. Commun.* **2010**, *46*, 677 – 685; i) H. M. L. Davies, J. Du Bois, J.-Q. Yu, *Chem. Soc. Rev.* **2011**, *40*, 1855 – 1856; j) K. Godula, D. Sames, *Science* **2006**, *312*, 67 – 72; k) L. Ackermann, R. Vicente, A. R. Kapdi, *Angew. Chem. Int. Ed.* **2009**, *48*, 9792 – 9826; *Angew. Chem.* **2009**, *121*, 9976 – 10011; l) G. P. Chiusoli, M. Catellani, M. Costa, E. Motti, N. D. Ca', G. Maestri, *Coord. Chem. Rev.* **2010**, *254*, 456 – 469.

[2] a) T. W. Lyons, M. S. Sanford, *Chem. Rev.* **2010**, *110*, 1147 – 1169; b) D.-H. Wang, M. Wasa, R. Giri, J.-Q. Yu, *J. Am. Chem. Soc.* **2008**, *130*, 7190 – 7191; c) S.-D. Yang, C.-L. Sun, Z. Fang, B.-J. Li, Y.-Z. Li, Z.-J. Shi, *Angew. Chem. Int. Ed.* **2008**, *47*, 1473 – 1476; *Angew. Chem.* **2008**, *120*, 1495 – 1498; d) M. D. K. Boele, G. P. F. van Strijdonck, A. H. M. de Vries, P. C. J. Kamer, J. G.; de Vries, P. W. N. M. van Leeuwen, *J. Am. Chem. Soc.* **2002**, *124*, 1586 – 1587; de Vries, P. W. N. M. van Leeuwen, *J. Am. Chem. Soc.* **2002**, *124*, 1586 – 1587; e) F. Li, T. Jiang, H. Cai, G. Wang, *Chin. J. Chem.* **2012**, *30*, 2041 – 2046; f) W. Shi, Z. Shi, *Chin. J. Chem.* **2014**, *32*, 974 – 980; g) X. Chen, K. M. Engle, D.-H. Wang, J.-Q. Yu, *Angew. Chem. Int. Ed.* **2009**, *48*, 5094 – 5115; *Angew. Chem.* **2009**, *121*, 5196 – 5217.

[3] a) K. S. Kanyiva, Y. Nakao, T. Hiyama, *Angew. Chem. Int. Ed.* **2007**, *46*, 8872 – 8874; *Angew. Chem.* **2007**, *119*, 9028 – 9030; b) Y. Nakao, K. S. Kanyiva, T. Hiyama, *J. Am. Chem. Soc.* **2008**, *130*, 2448 – 2449; c) M. Tobisu, I. Hyodo, N. Chatani, *J. Am. Chem. Soc.* **2009**, *131*, 12070 – 12071; d) I. Hyodo, M. Tobisu, N. Chatani, *Chem. Commun.* **2012**, *48*, 308 – 310; e) I. Hyodo, M. Tobisu, N. Chatani, *Chem. Asian J.* **2012**, *7*, 1357 – 1365; f) T. Yao, K. Hirano, T. Satoh, M. Miura, *Angew. Chem. Int. Ed.* **2012**, *51*, 775 – 779; *Angew. Chem.* **2012**, *124*, 799 – 803; g) K. Muto, J. Yamaguchi, A. Lei, K. Itami, *J. Am. Chem. Soc.* **2013**, *135*, 16384 – 16387.

[4] a) I. Özdemir, S. Demir, B. Çetinkaya, C. Gourlaouen, F. Maseras, C. Bruneau, P. H. Dixneuf, *J. Am. Chem. Soc.* **2008**, *130*, 1156 – 1157; b) S. Qi, H. Sato, S. Sugawara, Y. Inoue, *Org. Lett.* **2008**, *10*, 1823 – 1826; c) Y. Matsuura, M. Tamura, T. Kochi, M. Sato, N. Chatani, F. Kakiuchi, *J. Am. Chem. Soc.* **2007**, *129*, 9858 – 9859; d) L. Ackermann, A. Althammer, R. Born, *Angew. Chem. Int. Ed.* **2006**, *45*, 2619 – 2622; *Angew. Chem.* **2006**, *118*, 2681 – 2685; e) F. Kakiuchi, Y. Matsuura, S. Kan, N. Chatani, *J. Am. Chem. Soc.* **2005**, *127*, 5936 – 5945; f) F. Kakiuchi, S. Kan, K. Igi, N. Chatani, S. Murai, *J. Am. Chem. Soc.* **2003**, *125*, 1698 – 1699; g) S. Oi, Y. Ogino, S. Fukita, Y. Inoue, *Org. Lett.* **2002**, *4*, 1783 – 1785; h) S. Oi, S. Fukita, N. Hirata, N. Watanuki, S. Miyano, Y. Inoue, *Org. Lett.* **2001**, *3*, 2579 – 2581; i) P. B. Arockiam, C. Bruneau, P. H. Dixneuf, *Chem. Rev.* **2012**, *112*, 5879 – 5918.

[5] a) S. H. Wiedemann, J. C. Lewis, J. A. Ellman, R. G. Bergman, *J. Am. Chem. Soc.* **2006**, *128*, 2452 – 2462; b) J. C. Lewis, J. Y. Wu, R. G. Bergman, J. A. Ellman, *Angew. Chem. Int. Ed.* **2006**, *45*, 1589 – 1591; *Angew. Chem.* **2006**, *118*, 1619 – 1621; c) L. Shi, Y.-Q. Tu, M. Wang, F.-M. Zhang, C.-A. Fan, Y.-M. Zhao, W.-J. Xia, *J. Am. Chem. Soc.* **2005**, *127*, 10836 – 10837; d) K. Ueura, T. Satoh, M. Miura, *Org. Lett.* **2005**, *7*, 2229 – 2231; e) R. B. Bedford, M. E. Limmert, *J. Org. Chem.* **2003**, *68*, 8669 – 8682; f) S. Oi, S. Fukita, Y. Inoue, *Chem. Commun.* **1998**, 2439 – 2440; g) G. Song, F. Wang, X. Li, *Chem. Soc. Rev.* **2012**, *41*, 3651 – 3678; h) D. A. Colby, R. G. Bergman, J. A. Ellman, *Chem. Rev.* **2010**, *110*, 624 – 655.

[6] a) C. Bolm, J. Legros, J. Le Paih, L. Zani, *Chem. Rev.* **2004**, *104*, 6217 – 6254; b) C.-L. Sun, B.-J. Li, Z.-J. Shi, *Chem. Rev.* **2011**, *111*, 1293 – 1314; c) A. A. Kulkarni, O. Daugulis, *Synthesis* **2009**, 4087 – 4109; d) Y. Huang, D. Guan, L. Wang, *Chin. J. Chem.* **2014**, *32*, 1294 – 1298; e) E. Nakamura, N. Yoshikai, *J. Org. Chem.* **2010**, *75*, 6061 – 6067; f) N. Yoshikai, A. Matsumoto, J. Norinder, E. Nakamura, *Angew. Chem. Int. Ed.* **2009**, *48*, 2925 – 2928; *Angew. Chem.* **2009**, *121*, 2969 – 2972.

[7] a) D. L. Davies, O. Al-Duaij, J. Fawcett, M. Giardiello, S. T. Hilton, D. R. Russell, *Dalton Trans.* **2003**, 4132 – 4138; b) T. Satoh, M. Miura, *Chem. Eur. J.* **2010**, *16*, 11212 – 11222; c) Y. Shen, G. Liu, Z. Zhou, X. Lu, *Org. Lett.* **2013**, *15*, 3366 – 3369; d) Z. Shi, D. C. Koester, M. Boultadakis-Arapinis, F. Glorius, *J. Am. Chem. Soc.* **2013**, *135*, 12204 – 12207; e) J. Ryu, K. Shin, S. H. Park, J. Y. Kim, S. Chang, *Angew. Chem.* **2012**, *124*, 10042 – 10046; f) A. G. Algarra, W. B. Cross, D. L. Davies, Q. Khamker, S. A. Macgregor, C. L. McMullin, K. Singh, *J. Org. Chem.* **2014**, *79*, 1954 – 1970.

[8] X. Zhang, Z. Qi, X. Li, *Angew. Chem. Int. Ed.* **2014**, *53*, 10794 – 10798.

[9] U. Sharma, Y. Park, S. Chang, *J. Org. Chem.* **2014**, *79*, 9899 – 9906.

[10] a) J. Kwak, M. Kim, S. Chang, *J. Am. Chem. Soc.* **2011**, *133*, 3780 – 3783; b) J. Jeong, P. Patel, H. Hwang, S. Chang, *Org. Lett.* **2014**, *16*, 4598 – 4601; c) H. Hwang, J. Kim, J. Jeong, S. Chang, *J. Am. Chem. Soc.* **2014**, *136*, 10770 – 10776; d) T. Shibata, Y. Matsuo, *Adv. Synth. Catal.* **2014**, *356*, 1516 – 1520.

[11] a) D. E. Stephens, J. Lakey-Beitia, A. C. Atesin, T. A. Ateşin, G. Chavez, H. D. Arman, O. V. Larionov, *ACS Catal.* **2015**, *5*, 167 – 175; b) H. Konishi, S. Kawamorita, T. Iwai, P. G. Steel, T. B. Marder, M. Sawamura, *Chem. Asian J.* **2014**, *9*, 434 – 438; c) N. Boudet, J. R. Lachs, P. Knochel, *Org. Lett.* **2007**, *9*, 5525 – 5528.

[12] a) N. Guimond, C. Gouliaras, K. Fagnou, *J. Am. Chem. Soc.* **2010**, *132*, 6908 – 6909; b) N. Guimond, S. I. Gorelsky, K. Fagnou, *J. Am. Chem. Soc.* **2011**, *133*, 6449 – 6457; c) S. Rakshit, C. Grohmann, T. Besset, F. Glorius, *J. Am. Chem. Soc.* **2011**, *133*, 2350 – 2353; d) F. W. Patureau, F. Glorius, *Angew. Chem. Int. Ed.* **2011**, *50*, 1977 – 1979; *Angew. Chem.* **2011**, *123*, 2021 – 2023.

[13] a) J. Xiao, X. Li, *Angew. Chem. Int. Ed.* **2011**, *50*, 7226 – 7236; *Angew. Chem.* **2011**, *123*, 7364 – 7375; b) D. Chen, G. Song, A. Jia, X. Li, *J. Org. Chem.* **2011**, *76*, 8488 – 8494.

[14] a) G. Song, D. Chen, Y. Su, K. Han, C.-L. Pan, A. Jia, X. Li, *Angew. Chem. Int. Ed.* **2011**, *50*, 7791 – 7796; *Angew. Chem.* **2011**, *123*, 7937 – 7942; b) X. Li, A. R. Chianese, T. Vogel, R. H. Crabtree, *Org. Lett.* **2005**, *7*, 5437 – 5440.

[15] a) K. Pati, R.-S. Liu, *Chem. Commun.* **2009**, 5233 – 5235; b) B. Li, J. Ma, N. Wang, H. Feng, S. Xu, B. Wang, *Org. Lett.* **2012**, *14*, 736 – 739.

[16] a) Y. Tan, J. F. Hartwig, *J. Am. Chem. Soc.* **2010**, *132*, 3676 – 3677; b) L. Li, W. W. Brennessel, W. D. Jones, *Organometallics* **2009**, *28*, 3492 – 3500.

[17] Gaussian 09, Revision D.01, M. J. Frisch, G. W. Trucks, H. B. Schlegel, G. E. Scuseria, M. A. Robb, J. R. Cheeseman, G. Scalmani, V. Barone, B. Mennucci, G. A. Petersson, H. Nakatsuji, M. Caricato, X. Li, H. P. Hratchian, A. F. Izmaylov, J. Bloino, G. Zheng, J. L. Sonnenberg, M. Hada, M. Ehara, K. Toyota, R. Fukuda, J. Hasegawa, M. Ishida, T. Nakajima, Y. Honda, O. Kitao, H. Nakai, T. Vreven, J. A. Montgomery, Jr., J. E. Peralta, F. Ogliaro, M. Bearpark, J. J. Heyd, E. Brothers, K. N. Kudin, V. N. Staroverov, R. Kobayashi, J. Normand, K. Raghavachari, A. Rendell, J. C. Burant, S. S. Iyengar, J. Tomasi, M. Cossi, N. Rega, J. M. Millam, M. Klene, J. E. Knox, J. B. Cross, V. Bakken, C. Adamo, J. Jaramillo, R. Gomperts, R. E. Stratmann, O. Yazyev, A. J. Austin, R. Cammi, C. Pomelli, J. W. Ochterski, R. L. Martin, K. Morokuma, V. G. Zakrzewski, G. A. Voth, P. Salvador, J. J. Dannenberg, S. Dapprich, A. D. Daniels, Ö. Farkas, J. B. Foresman, J. V. Ortiz, J. Cioslowski, D. J. Fox, Gaussian, Inc., Wallingford CT, **2009**.

[18] a) A. D. Becke, *J. Chem. Phys.* **1993**, *98*, 5648; b) C. Lee, W. Yang, R. G. Parr, *Phys. Rev. B* **1988**, *37*, 785.

[19] R. Peverati, D. G. Truhlar, *J. Phys. Chem. Lett.* **2012**, *3*, 117 – 124.

[20] a) R. Peverati, D. G. Truhlar, *Phys. Chem. Chem. Phys.* **2012**, *14*, 11363 – 11370; b) Y.-S. Lin, C.-W. Tsai, G.-D. Li, J.-D. Chai, *J. Chem. Phys.* **2012**, *136*, 154109; c) J. A. Steckel, *J. Phys. Chem. A* **2012**, *116*, 11643 – 11650; d) Y. Zhao, H. T. Ng, R. Peverati, D. G. Truhlar, *J. Chem. Theory Comput.* **2012**, *8*, 2824 – 2834; e) Z. Yu, Y. Lan, *J. Org. Chem.* **2013**, *78*, 11501 – 11507; S. Liu, H. Shen, Z. Yu, L. Shi, Z. Yang, Y. Lan, *Organometallics* **2014**, *33*, 6282 – 6285; Y. Xi, Y. Su, Z. Yu, B. Dong, E. J. McClain, Y. Lan, X.

Shi, *Angew. Chem. Int. Ed.* **2014**, *53*, 9817 – 9821; *Angew. Chem.* **2014**, *126*, 9975 – 9979.

[21] A. V. Marenich, C. J. Cramer, D. G. Truhlar, *J. Phys. Chem. B* **2009**, *113*, 6378 – 6396.

[22] a) Q. Zhang, H.-Z. Yu, Y.-T. Li, L. Liu, Y. Huang, Y. Fu, *Dalton Trans.* **2013**, *42*, 4175 – 4184; b) X.-S. Zhang, K. Chen, Z.-J. Shi, *Chem. Sci.* **2014**, *5*, 2146 – 2159; c) L. Liu, Y. Wu, T. Wang, X. Gao, J. Zhu, Y. Zhao, *J. Org. Chem.* **2014**, *79*, 5074 – 5081; d) W.-J. Chen, Z. Lin, *Organometallics* **2015**, *34*, 309 – 318; e) S. Yu, S. Liu, Y. Lan, B. Wan, X. Li, *J. Am. Chem. Soc.* **2015**, *137*, 1623 – 1631.

Received: January 22, 2015
Published online on June 8, 2015